We are IntechOpen,
the world's leading publisher of
Open Access books
Built by scientists, for scientists

4,800
Open access books available

122,000
International authors and editors

135M
Downloads

154
Countries delivered to

Our authors are among the

TOP 1%
most cited scientists

12.2%
Contributors from top 500 universities

CLARIVATE ANALYTICS
BOOK CITATION INDEX
INDEXED

WEB OF SCIENCE™

Selection of our books indexed in the Book Citation Index
in Web of Science™ Core Collection (BKCI)

Interested in publishing with us?
Contact book.department@intechopen.com

Numbers displayed above are based on latest data collected.
For more information visit www.intechopen.com

HRTEM Study on Resistive Switching ZrO$_2$ Thin Films and Their Micro-Fabricated Thin Films

Ying Li, Gaoyang Zhao, Zhibo Kou, Long Jin and Yajing Wang

Additional information is available at the end of the chapter

Abstract

For the next-generation nonvolatile memory material, the most promising candidate is resistive random access memory (RRAM) which is nonvolatile memory with high density, high speed, and low power consumption. Resistive switching (RS) behavior had been reported in various films including transition metal oxides, perovskite, and chalcogenide. For further application, it is still a challenge to fabricate nanostructures of RS material. Micro-fabrication method involves traditional lithography, chemical etching, electron beam direct writing, nano-imprint, and so on. However, the procedure and the cost of these methods are relatively complex and high for semiconductors process. In this chapter, we demonstrate a method for fabricating sub-micro ZrO$_2$ lattice by using sol-gel method combined with laser interference lithography and micro-analysis with high-resolution transmission electron microscopy (HRTEM).

Researchers used all kinds of techniques to investigate the mechanism such as conductive atomic force microscopy, HRTEM, and scanning electrical microscopy. Despite the extensive research, much of the underlying mechanism is still unclear and controversial. This task can be accomplished only with advanced measurement and technique such as in HRTEM, local conductive atomic force microscopy, and so on. HRTEM sample preparation method for array dots is also discussed. In our research, the bipolar RS behavior can be observed successfully in this structure. And HRTEM observation was used to study the interface between the layers. RRAM unit consists of a conductive atomic force microscope tip as an anode, a ZrO$_2$ lattice dot as RS material, and a copper electrode as a cathode.

**Keywords:** Resistive switching, HRTEM, Sample preparation

1. Introduction

The development of information technology has brought rapid changes to people's life. Resistive random access memory (RRAM), because of its fast response, high stability, low power consumption, with the traditional advantages of the semiconductor technology, has good compatibility, and according to scientists, is expected to become one of the next generations of memory [1-5]. In this chapter, by using shadow lithography and laser interference lithography, two kinds of methods to micro-fabricate the RS oxide film, it is suggested that the oxide film is suitable for micromachining process than using atomic force microscopy (AFM) in situ electrical measurement technique for fine-patterned films after the oxide film was studied by means of in situ micro area electrical performance. In this chapter, we used sol-gel method and chemical modification method for the preparation of a variety of ZrO_2 sol, and optimizing the good comprehensive properties of oxide RS material, through the analysis of the HRTEM studies of the oxide film [6-10].

2. Experiment

2.1. ZrO_2 thin films preparation

Photosensitive ZrO_2 films were fabricated with the metal alkoxide zirconium tetran-butoxide [$Zr(OC_4H_9)_4$], benzoylacetone (BzAcH), and ethanol (EtOH) in the molar ratio of Zr:BzAcH:EtOH at 1:1:40. After being mixed and refluxed for 2 to 3 hours, the photosensitive ZrO_2 solution was obtained. Then using dip-coating process, ZrO_2 organic films were formed on copper substrate. The copper substrates were fabricated by magnetic sputtering.
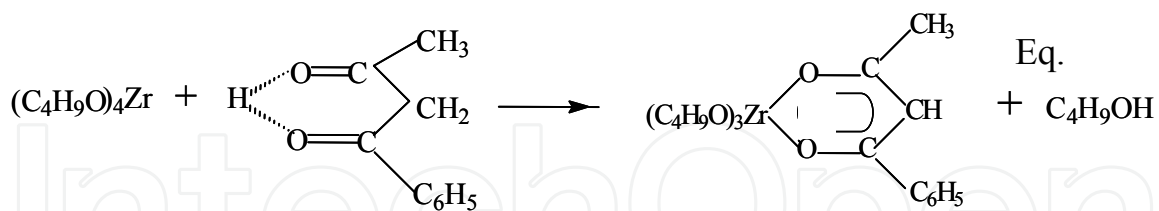
2.2. ZrO_2 lattice preparation

ZrO_2 lattice was fabricated by double exposures of two-beam laser interference through 90° rotation of the sample in its own plane between twice exposures with 350 nm Krypton ion laser. After laser exposure, the exposed part of ZrO_2 film is not soluble in leaching solution while the un-exposed part is still soluble. Therefore, ZrO_2 lattice can be obtained [11-14].

The UV–visible absorption spectra were measured and these spectra of the ZrO_2 films were dip-coated on quartz glass substrate. It was known that an absorption peak of BzAcH at 308 nm was due to the π-to-π^* transition. These peaks shift to 338 nm in the spectra of the ZrO_2 gel films. This red shift indicates the chelation between Zr^{4+} and BzAcH, and the reaction re-

sults in the partial replacement of the alkoxy group by β-diketone ligand [see Eq. (1)]. Fig. 1 also shows the AFM image of ZrO$_2$ films irradiated by a UV Krypton ion laser. The intensity of absorption peaks at around 338 nm decreases step by step with increasing irradiation time from 0 second to 400 seconds. These decreasing spectra showed that the chelate rings were dissociated by UV irradiation.
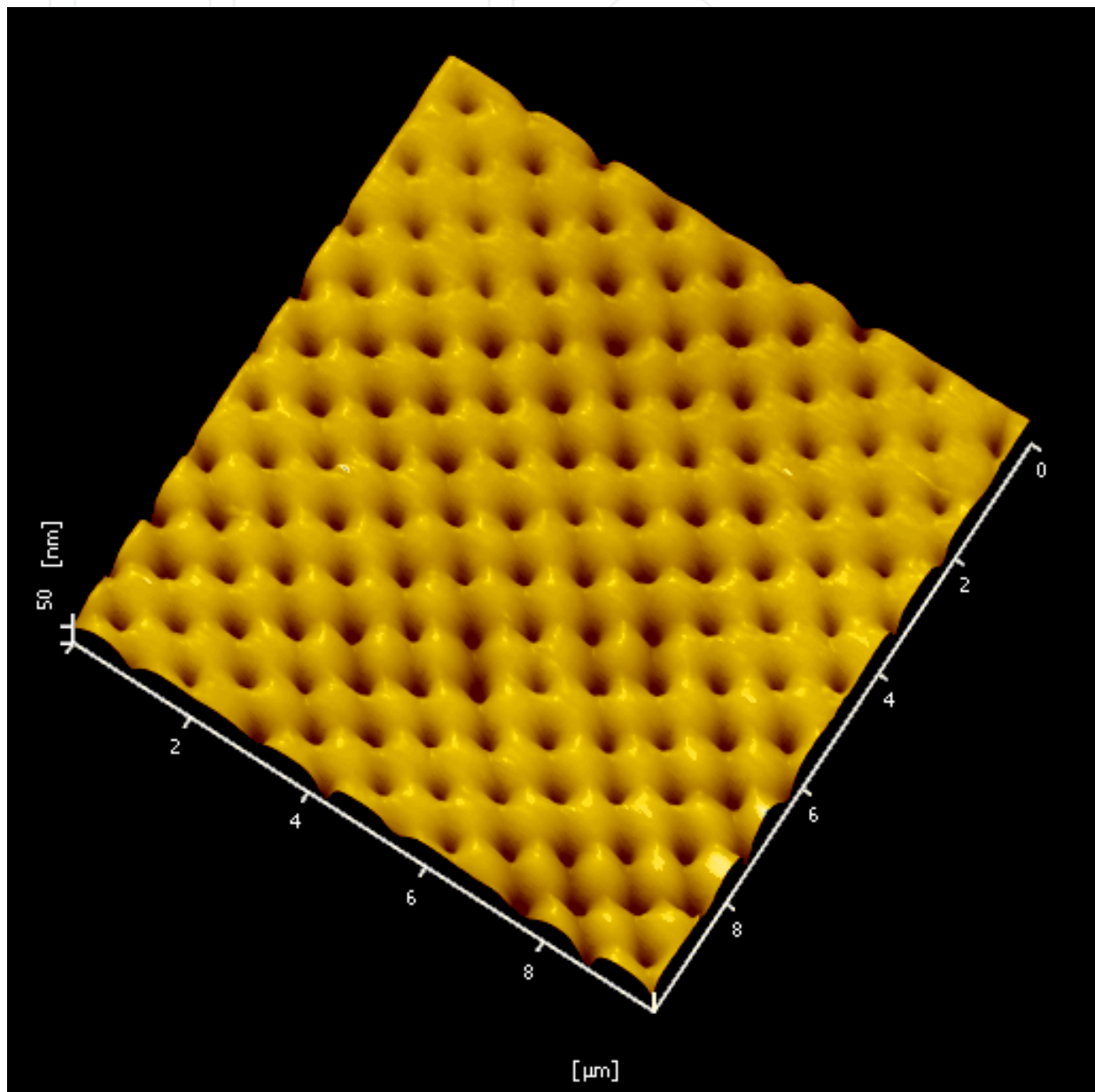

Figure 1. Observation of ZrO$_2$ lattice dot by AFM measurement systems.

2.3. I-V measurement with ZrO$_2$ thin films

Before the local conductive AFM (LC-AFM) measurement of the ZrO$_2$ lattice dots, a traditional I-V probe station measurement was carried out with the normal ZrO$_2$ thin film which

is made of the photosensitive ZrO_2 solution. This RS structure is formed with platinum (top electrode), ZrO_2 photosensitive film (RS layer), and copper (bottom electrode). The platinum top electrode is made by sputtering with shadow mask. The pattern of the shadow mask is periodic lattice dot with a diameter of 2 mm.

2.4. I-V measurement with ZrO_2 lattice

This LC-AFM measurement system consists an atomic force microscope (AFM, Seiko Instruments Inc, SPI3800N/SPA-400) with a resolution of 0.1 nm in x–y directions and 0.01 nm in the z direction and a Keithly 2400 I-V source meter (Keithly, USA.). The silicon tips (PPP-CONT, Nanosensors) were coated by sputtering deposition with a 25 nm thick double layer of chromium and platinum/Iridium (Pt/Ir) with an initial 20 nm radius. In our LC-AFM measurement study, RRAM unit consists of a conductive atomic force microscope tip as an anode, a ZrO_2 lattice dot as RS material, and a copper electrode as a cathode. In order to identify the RS properties of ZrO_2 array dot, the Pt/Ir conductive atomic force microscope tip is tightly positioned at the center of one of the dots. During the LC-AFM measurement, Pt/Ir conductive probe and the base of the LC-AFM are connected to Keithly 2400 meter to apply the excitation signal and record voltage and current response of the RS array dots. When the voltages from Keithly 2400 meter are applied to the Pt/Ir conductive AFM tip and the bottom electrode of the sample, the current flow occurs through the cantilever and goes back to the Keithly 2400 meter. Then a local I-V curve can be obtained.

In order to solve the influence from huge contact resistance between the Pt/Ir conductive atomic force microscope tip and a single ZrO_2 array dot, a platinum layer was spread on the whole ZrO_2 lattice by sputtering. In this way, the contact can be improved.

2.5. HRTEM sample preparation

The HRTEM observation was carried out by HRTEM (JEOL 3010, Japan). The diagram of sample preparation process is shown in Fig. 2. In Fig. 2(a), we cut some tiny part from the platinum-covered sample which can achieve I-V curves by LC-AFM systems for HRTEM observations.

Two tiny parts were pasted by AB glue face-to-face. AB glue should be used as less as possible because the more AB glue used the worse ion milling would be. And this unit was milled by hand in x direction as smooth as possible. When the thickness in z direction decreases down to less than 1 μm, this unit can be pasted to nickel (Ni) grid. This will be ready for Argon ions milling. A cross-section sample of Pt/ZrO_2 lattice dot/Cu unit was milled by the low-angle Argon milling machine (Gatan, USA). The milling angle was less than 8°. Microstructural analysis was done on the basis of HRTEM observations. It is well known that the preparation of good specimens for high-resolution transmission microscopy is a very important process. The milling angle of Argon ions was less than 8° for the reasons of the damage from Argon ions. The transparent area to electrons can be widened if the Argon ions milling angle was small. However, it cannot mill if the milling angle was less than 3°. The ideal milling angle of Argon ions was between 4° and 8°.
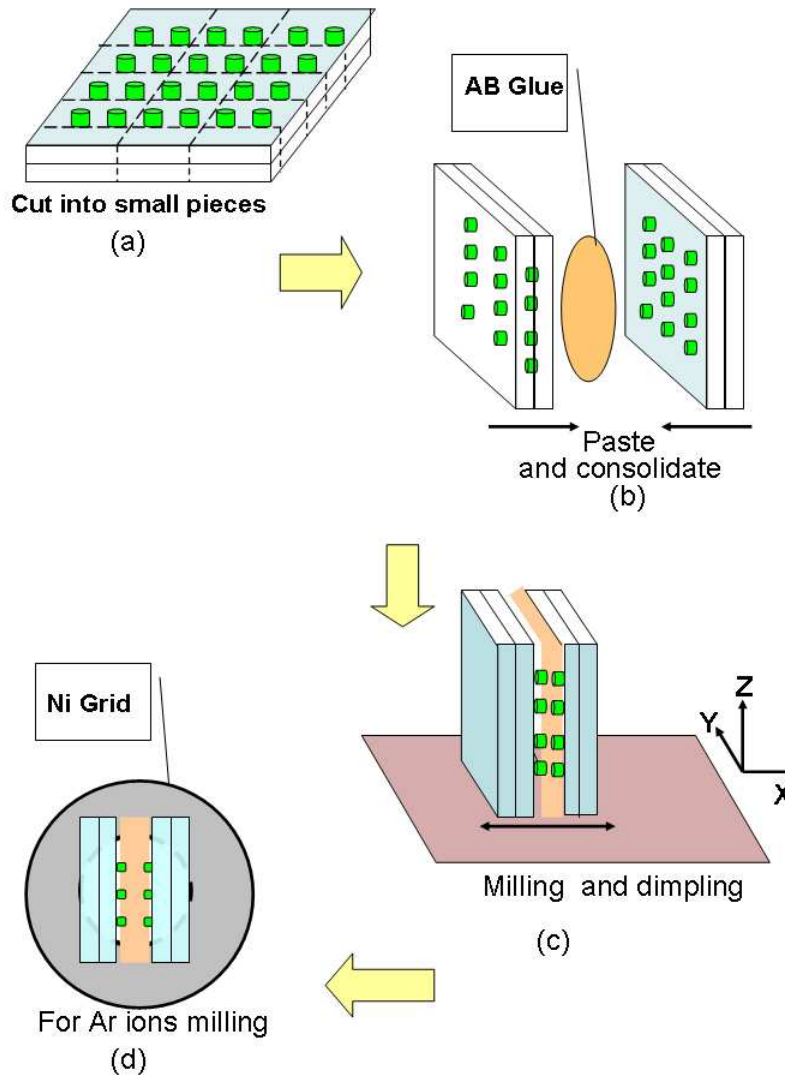
Figure 2. Illustration of HRTEM samples preparation process.

3. Discussion and results

3.1. Normal probe station I-V curves

For the electrical measurements, probes contact top electrode (Cu) and bottom electrode SnO$_2$:Sb (ATO), respectively. The bottom electrode was grounded. In Fig. 3, it shows the I-V characteristics of the Cu/ZrO$_2$/ATO structure after fifty times of I-V measurements cycles. The current compliance (CC) is applied to 10 mA during I-V sweep. When the voltage goes to 0.5 V, the current increases rapidly which means the OFF state switches to the ON state. During the I-V sweep at negative side, when the voltage goes to -1.4 V, the current decreases rapidly which means the ON state switches to the OFF state. This behavior can be repeated more than fifty times.
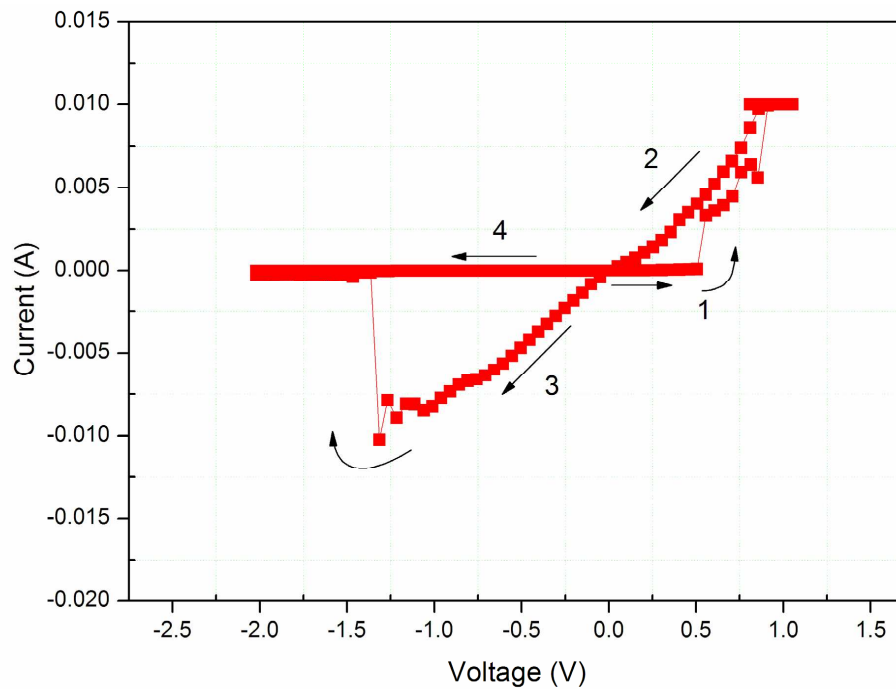
Figure 3. I-V curve of the Cu/ZrO$_2$/ATO structure after fifty cycles.

Bipolar RS characterization was stable for ZrO$_2$ thin film in the structure unit. Normally, the voltage sweeps start from 0 V and go to the positive side (1 V) and goes back to 0 V. Resistance switches from high resistance state (R$_H$) to low resistance state (R$_L$) and it is called SET process. And then the voltage sweeps from 0 V to the negative side (-2 V) and goes back to 0 V. Resistance switches from R$_L$ to R$_H$ and it is called RESET process. When the voltage swept at -0.5 V, R$_L$ was 70 Ω and R$_H$ was 100 KΩ. This behavior can be repeated hundreds of times. The CC is applied with 10 mA. The highest ratio of R$_H$:R$_L$ can reach to 10^4.

During the RESET operation, the interesting thing we found is that R$_H$ varied when we changed the RESET voltage. R$_H$ decreased when the RESET voltage value decreased. For I-V curve in Fig. 3, voltage sweep started from 0 V to the -2 V and then from -2 V to 0 V during the RESET process. When the voltage swept at -0.5 V, R$_L$ was 100 Ω and R$_H$ was 250 KΩ. This behavior can be repeated more than several times. The CC is applied with 10 mA. The highest ratio of R$_H$:R$_L$ can reach to 10^4.

3.2. Local I-V curves by LC-AFM measurement systems

During the LC-AFM measurement, the parameters of I Gain and P Gain should be adjusted. The value of P Gain should be set as one-third of I Gain value. The Pt/Ir conductive coating could be switched off when the value of Force Reference is too small. This value should be set from -1 nm to -4 nm. The sweep voltage can be set from -25 V to 25 V. The height of array dot A (ΔZ) is about 61 nm and dot B (ΔZ) is about 58 nm. The diameter of dot A is about 1.2 μm and that of dot B is about 1.1 μm. Local I-V curves are measured while the LC-AFM image was scanning. The CC is applied to 100 μA during I-V sweep. When the voltage goes to

18 V, the current increases rapidly which means the OFF state switches to the ON state. During the I-V sweep at negative side, when the voltage goes to -5.0 V, the current decreases rapidly which means the ON state switches to the OFF state. In order to make sure that the array dot is not shifted during the LC-AFM measurement, an AFM image scan is very necessary after the local I-V measurement is finished.

A platinum film of 30 nm thickness was sputtered on ZrO_2 lattice dot. Fig. 4 is a local I-V curve which is also measured while the LC-AFM image was scanning. The CC is applied to 100 μA during I-V sweep. When the voltage goes to 0.8 V, the current increases rapidly which means the OFF state switches to the ON state. During the I-V sweep at negative side, when the voltage goes to -2.2 V, the current decreases rapidly which means the ON state switches to the OFF state.
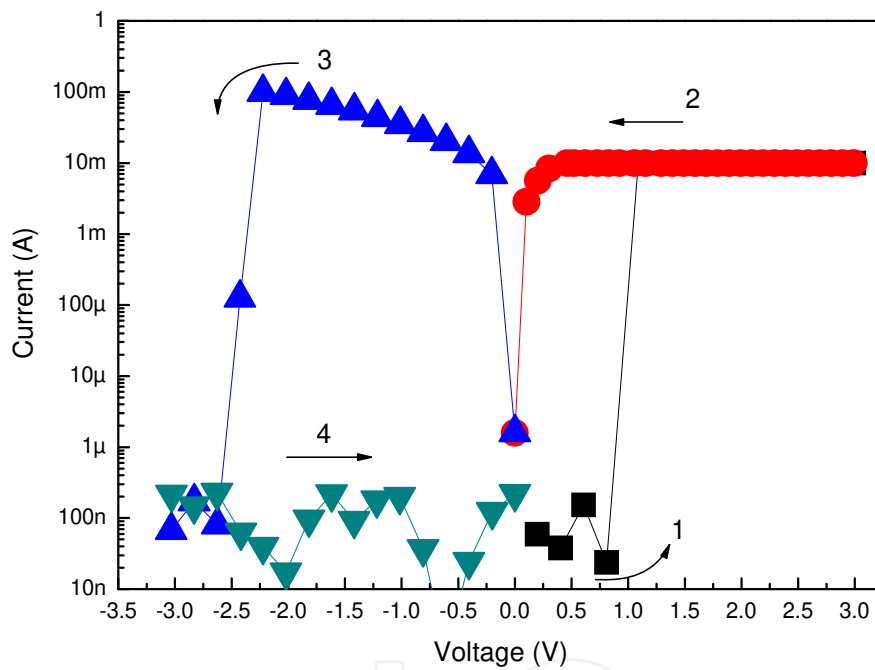

Figure 4. A local I-V curve which is measured while the LC-AFM image was scanning.

3.3. HRTEM observations

We took one unit of samples for TEM observations in which the ZrO_2 thin film in the structure was annealed at 300°C. Microstructural analysis has been done on the basis of TEM observations. Fig. 5 shows the interface image of $Cu/ZrO_2/ATO$ structure in which the ZrO_2 thin film was annealed at 300°C. The bottom electrode (BE) is ATO film and the thickness is about 400 nm. The ZrO_2 work layer is about 200 nm thick and it is amorphous according to the selected area diffraction pattern. In Fig. 5, it is shown that copper ions are penetrated into the ZrO_2 layer. It can be proved by the Fast Fourier Transform patterns. According to the filament formation mechanism, resistance reduction in the devices is due to the existing

copper to form conducting copper-rich pathways. An opposite bias takes the existing copper back to the copper electrode to its high resistance state [15-19].
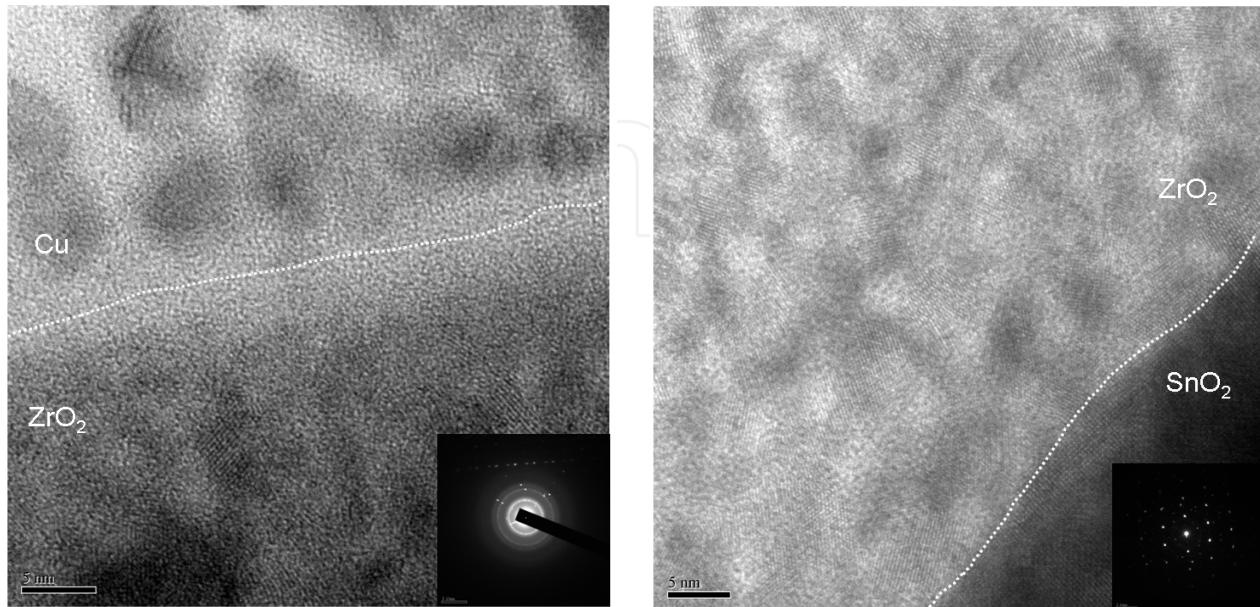

Figure 5. HRTEM image of Cu/ZrO$_2$/ATO structure.

Fig. 6(a) shows the interface image of Pt/ZrO$_2$ lattice dot/Cu sandwiched structure. Two lattice dots were seen in this figure, which are labeled as A and B. These two dots were not similar in size. This phenomenon was also seen in the rest of the HRTEM sample observations. The diameter of dot A is around 800 nm while that of dot B is around 700 nm. This is not agreeing with the LC-AFM image results. Through LC-AFM image observation, it is shown that the ZrO$_2$ array dots are even and in the same diameter range of about 1 μm. This is because when the HRTEM sample was milling manually in the first stage, it was difficult to keep the milling plane vertical to the ZrO$_2$ array plane. This is shown in Fig. 7(a) as the ideal case. It was always tilted a little bit which was perhaps due to the milling stage, sandpaper, or movement by hands. This is shown in Fig. 7(b) which is the practical case. For the conventional TEM specimen preparation techniques such as polished milling, the milling direction is controlled only by hands. Therefore, in the future HRTEM observation, an automatic monitor for sample milling system is necessary.

This HRTEM image is accepted for interface analysis. In inset of Fig. 6(a), it shows the selected area diffraction pattern of platinum, ZrO$_2$, and copper which are corresponding to polycrystalline, amorphous, and polycrystalline behaviors, respectively. Fig. 6(a) shows the HRTEM image of copper layer and Fig. 6(c) shows the interface between ZrO$_2$ array dot and platinum layer. In HRETM images, copper ions filaments were not found in the amorphous ZrO$_2$ array dot. Therefore, it is possible that the Redox process could have happened in the interface between copper layer and ZrO$_2$ array dot.
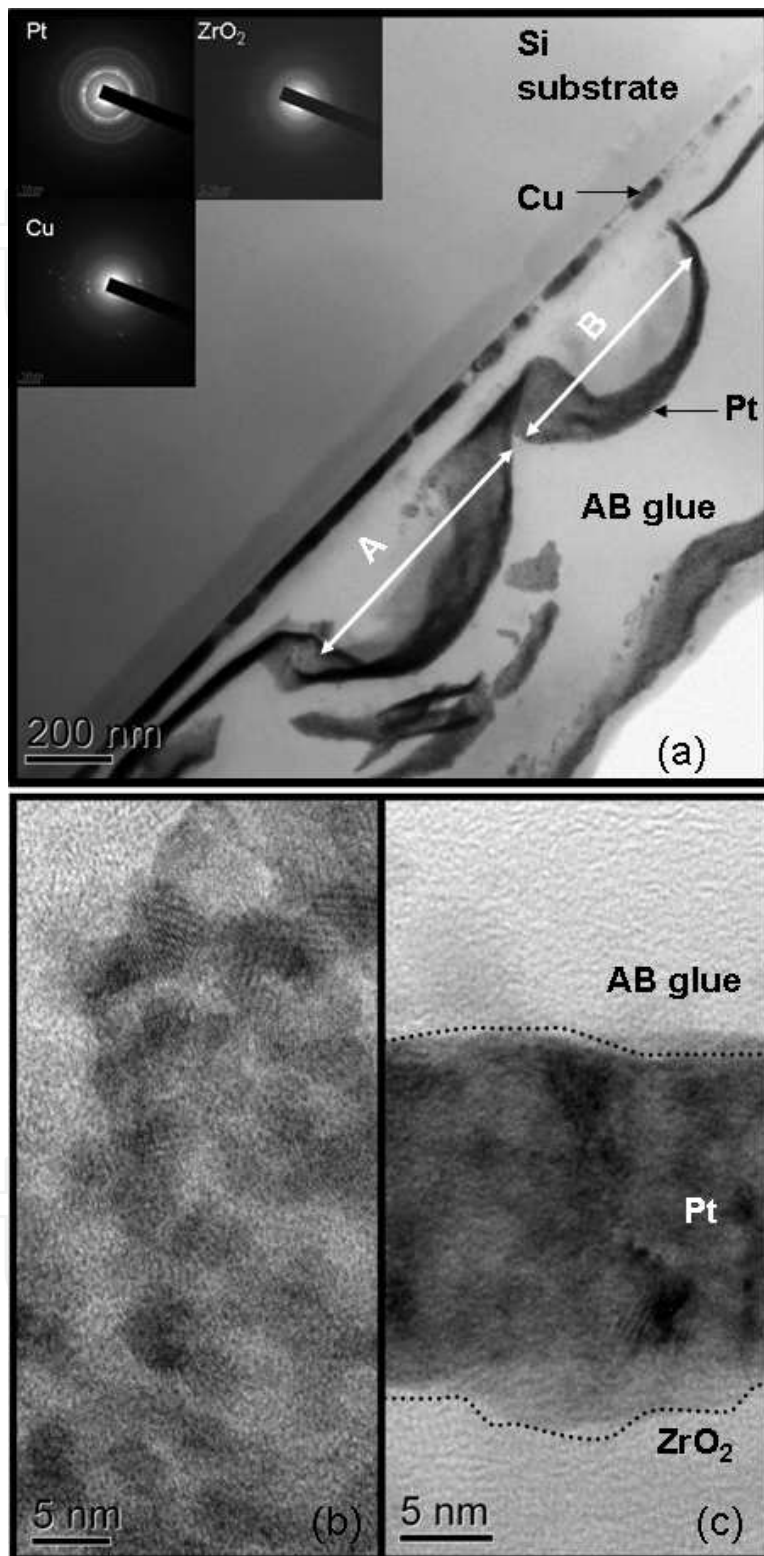
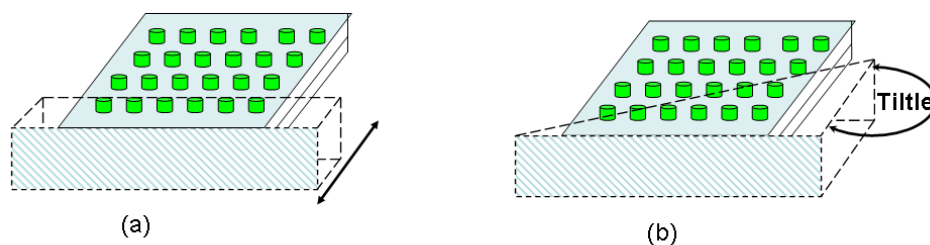**Figure 6.** HRTEM interface image of Pt/ZrO$_2$ lattice dot/Cu structure.

Figure 7. HRTEM sample milling diagrams.

4. Conclusion

We fabricated ZrO_2 thin films after annealing at 300°C through sol-gel deposition. Reproducible I-V curves can be obtained with these samples at room temperature (300 K). The ZrO_2 thin film annealed at 300°C in Cu/ZrO_2/ATO device can also be operated in RS sweeps cycles. In summary, we fabricated TiO_2 thin films by sol-gel deposition. Successful Cu/ZrO_2/ATO structure device in which ZrO_2 thin film was calcined at 300°C can be obtained. The bipolar RS behavior was observed and the ratio of R_{off}:R_{on} can be reached to 10^4. We also investigated the switching device of Pt/ZrO_2 lattice dot/Cu sandwiched structure by HRTEM.

Acknowledgements

Author details

Ying Li[1*], Gaoyang Zhao[2], Zhibo Kou[3], Long Jin[2] and Yajing Wang[2]

*Address all correspondence to: liying@xaut.edu.cn

1 Advanced Material Analysis Center, Xi'an University of Technology, Xi'an, Shaanxi, China

2 Material Science and Engineering School, Xi'an University of Technology, Xi'an, Shaanxi, China

3 Northwest Electric Power Design Institute of China Power Engineering Consulting Group, Xi'an, Shaanxi, China

References

[1] B.J. Choi, D.S. Jeong, S.K. Kim, et al. Temperature influence and reset voltage study of bipolar resistive switching behaviour in ZrO$_2$ thin films. *J Appl Phys*. 98 (2005), 037715-037725.

[2] H. Shima, Y. Tamai. Top electrode effects on resistive switching behavior in CuO thin films. *Microelectron J*. 40 (2009), 628-632.

[3] M.J. Rozenberg, I.H. Inoue, M.J. Sanchez. Nonvolatile memory with multilevel switching: A basic model. *Phys Rev Lett*. 92 (17) (2004), 178302-178306.

[4] X. Guo, C. Schindler, S. Menzel, R. Waser. Understanding the switching-off mechanism in Ag+ migration based resistively switching model systems. *Appl Phys Lett*. 91 (13) (2007), 133513-133516.

[5] R. Waser. Resistive non-volatile memory devices. *Microelectron Eng*. 86 (2009), 1925-1928.

[6] Y. Li, G. Zhao, J. Su, E. Shen, Y. Ren. Top electrode effects on 6 resistive switching behavior in CuO thin films. *Appl Phys A*. 104 (2011), 1069-1073.

[7] C. Gopalan, M.N. Kozicki, S. Bhagat. *J Non-Crystal Solids*. 353 (2007), 1844-1848.

[8] X. Zhi, G. Zhao, T. Zhu, Y. Li. The morphological, optical and electrical properties of SnO$_2$:F thin films prepared by spray pyrolysis. *Surf Interface Anal*. 40 (2008), 67-70.

[9] S. Pulston, P.M. Parlett, P. Stones, M. Bowker. Surface Oxidation and Reduction of CuO and Cu$_2$O Studied Using XPS and XAES. *Sur Interface Anal*. 24 (1996), 811-820.

[10] M.C. Lopez, B. Galiana, C. Algora, I. Rey-Stolle, M. Gabas, J.R. Ramos-Barrado. Chemical characterization by XPS of Cu/Ge ohmic contacts to n-GaAs, *Applied Surface Science*, 253 (2007), 5062-5066.

[11] C.D. Wagner,W.M. Riggs, L. E. Davis, J.F. Moulder, G. E. Muilenberg. Handbook of X-ray Photoelectron Spectroscopy. Perkin-Elmer, Minnesota, 1979.

[12] X. Wu, P. Zhou, J. Li, et al. Reproducible unipolar resistance switching in stoichiometric ZrO$_2$ films.*Appl Phys Lett*. 90 (2007), 183507-183511.

[13] D.Lee. Resistance switching of copper doped MoOx films for nonvolatile memory applications. Appl Phys Lett. 90 (2007), 122104.

[14] C.C. Lin, B.C. Tu. Resistive switching mechanisms of V-doped SrZrO$_3$ memory films. *IEEE Electron Device Lett*, 27 (2006), 725–727.

[15] D.S. Jeong, C.S. Hwang. Reasons for obtaining an optical dielectric constant from the Poole–Frenkel conduction behavior of atomic-layer-deposited HfO2 films. *Appl Phys Lett*. 86 (2005), 072903.

[16] C. Schindler, S.C.P. Thermadam, R. Waser, M.N. Kozicki. Bipolar and unipolar resistive switching in Cu-doped SiO$_2$. *IEEE Trans Electr Dev*. 30 (1) (2007), 2762.

[17] A. Sawa, T. Fujii, M. Kawasaki. Interface resistance switching at a few nanometer thick perovskite manganite active layers. *Appl Phys Lett*. 88 (2006),1-3.

[18] K.M. Kim, B.J. Choi, Y.C. Shin, S. Choi, C.S. Hwang. Anode-interface localized filamentary mechanism in resistive switching of TiO$_2$ thin films. *Appl Phys Lett*. 91 (2007), 012907.

[19] C. Kügeler, R. Rosezin, E. Linn, R. Bruchhaus, R. Waser. Materials, technologies, and circuit concepts for nanocrossbar-based bipolar RRAM. *Appl* Phys A. 102 (2011), 791-809.